ACADEMIC PRESS

Available online at www.sciencedirect.com
SCIENCE DIRECT®

NeuroImage

NeuroImage 20 (2003) 512–519

www.elsevier.com/locate/ynimg

Characterization of sexual dimorphism in the human corpus callosum

Abraham Dubb,* Ruben Gur,[1] Brian Avants,[2] and James Gee[3]

Departments of Bioengineering, Psychiatry, and Radiology, University of Pennsylvania, Philadelphia, PA 19104-6389, USA

Received 11 December 2002; revised 2 May 2003; accepted 8 May 2003

Abstract

Despite decades of research, there is still no agreement over the presence of gender-based morphologic differences in the human corpus callosum. We approached the problem using a highly precise computational technique for shape comparison. Starting with a prospectively acquired sample of cranial MRIs of healthy volunteers (age ranges 18–84), the variations of individual callosa are quantified with respect to a reference callosum shape in the form of Jacobian determinant maps derived from the geometric transformations that map the reference callosum into anatomic alignment with the subject callosa. Voxelwise *t* tests performed over the determinant values demonstrated that females had a larger splenium than males ($P < 0.001$ uncorrected for multiple comparisons) while males possessed a larger genu ($P < 0.001$). In addition, pointwise Pearson plots using age as a correlate showed a different pattern of age-related changes in male and female callosa, with female splenia tending to expand more with age, while the male genu tended to contract. Our results demonstrate significant morphologic differences in the corpus callosum between genders and a possible sex difference in the neuro-developmental cycle.

1. Introduction

Differences in higher cortical functioning between males and females have been the target of considerable investigation for a number of decades. Cognitive and functional imaging studies have suggested a greater degree of hemispheric lateralization in males compared to females, while females displayed increased bilateral hemispheric activity for a variety of cognitive tasks (Harshman and Remington, 1976; McGlone, 1980; Bryden, 1979; Kimura and Harshman, 1984; Shaywitz et al., 1995). These studies seem to suggest enhanced interhemispheric communication in females and have motivated investigation into sexual dimorphism of the corpus callosum. The corpus callosum is the brain's largest white-matter tract and the primary means of communication between the two cerebral hemispheres, prompting investigators to hypothesize that differences in callosal size exist between males and females. Most investigators have examined the shape and size of the midsagittal section of the callosum as a surrogate for the structure's overall shape. To date, however, no consensus has been reached on the presence of such gender-based differences in the callosum. De Lacoste and Holloway (1982) reported in 1982 that the female splenium was more bulbous than the tubual male splenium. Follow-up studies by De Lacoste et al. (1986), Yoshi et al. (1986), and Allen et al. (1991) all found increased size in the female splenium. In contrast, Weis and colleagues (Weis et al., 1989), Going and Dixson (1990), and Witelson (1985) all reported no such differences between the callosa of males and females.

One possible reason for this prevailing controversy may be the lack of standards in callosal analysis. While cross-sectional area and callosal length are the more traditional indices reported in gender studies, there is little agreement over how to normalize these indices. Furthermore, gross dimensional measures will miss regional shape variations in callosa. Some investigators have divided the callosa into partitions and compared the area of corresponding partitions between study groups (Witelson, 1985). The difficulty here is that the selection of the partitioning method is arbitrary and subpartition size differences may escape detection.

We used template deformation morphometry (TDM) (Machado and Gee, 1998; Machado et al., 2000; Davatzikos

* Corresponding author.
E-mail address: adubb@grasp.cis.upenn.edu (A. Dubb).
[1] *E-mail address:* gur@bblmail.psycha.upenn.edu (R. Gur).
[2] *E-mail address:* avants@grasp.cis.upenn.edu (B. Avants).
[3] *E-mail address:* gee@rad.upenn.edu (J. Gee).

1053-8119/03/$ – see front matter © 2003 Elsevier Inc. All rights reserved.
doi:10.1016/S1053-8119(03)00313-6

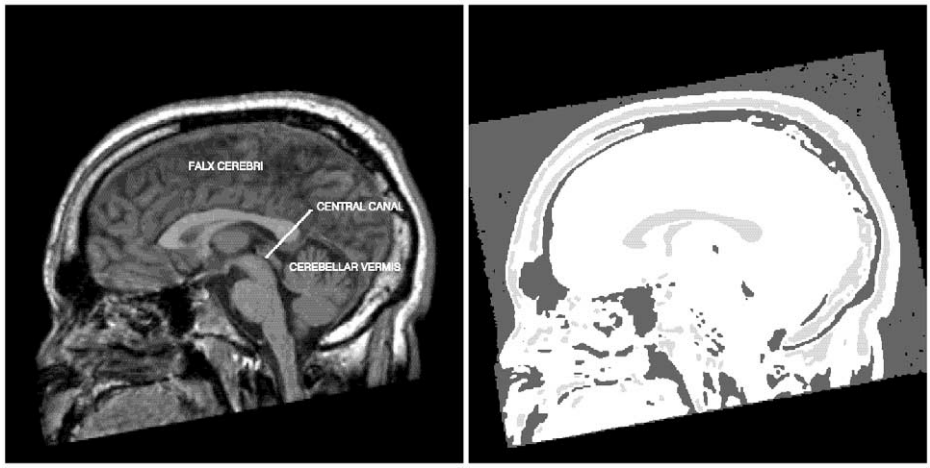

Fig. 1. Raw mid-sagittal image (left) and segmentation mask (right). The raw image on the left shows the three anatomical structures which signify a mid-sagittal slice. The frequent presence of the interventricular septum within this slice complicates segmentation. On the right, a successful *k*-means probability-based segmentation image which shows the corpus callosum as a solitary region.

et al., 1996), which avoids many of the pitfalls associated with more traditional measures of the callosum. By registering each subject to a template callosum and normalizing over that callosum's area, we avoid the issue of normalizing measurements to some arbitrary index of overall brain size (Bermudez and Zatorre, 2001). In addition, TDM gives a pointwise measure of expansion or contraction and so is more sensitive to regional morphologic differences than any partitioning method. Finally, TDM is a general strategy for comparing shape, and so can be used to analyze any part of the brain, indeed the whole brain, in principle.

2. Materials and methods

2.1. Subjects and data acquisition

The Schizophrenia Center at the University of Pennsylvania maintains a database containing hundreds of prospectively accrued cranial MRIs of psychiatric patients and healthy volunteers. The sample selection procedures have been detailed in Shtasel et al. (1991), the MRI acquisition protocol has been described in detail in Gur et al. (1999b), and results of volumetric segmentation analysis for this sample have been reported (Gur et al., 1998, 1999a, 1999b). Our selection criteria specified right handed participants with a diagnosis of healthy control, for whom a high-resolution spoiled-gradient recalled pulse sequence (SPGR) scan was available. SPGR scans were acquired on a 1.5 T scanner (Signa; General Electric Co., Milwaukee, WI) using the following parameters: flip angle of 35°, repetition time of 35 ms, echo time of 6 ms, field of view of 24 cm, 1 repetition, 1 mm slice thickness, and no interslice gaps. Transaxial images were in planes parallel to the orbitomeatal line, with resolution of 0.9375×0.9375 mm^2 (Gur et al., 1999b).

2.2. Reslicing

Our goal in reslicing the brain volumes was to obtain the most precise mid-sagittal image possible. This procedure was necessitated by the fact that most participants had tilted their heads slightly to the left or right side during the scan. We adopted the reslicing protocol used by the Schizophrenia Center by performing the following steps: first, the volume was rotated around the anterior-posterior (AP) axis until the eyeballs were positioned in the same horizontal plane. Next, an approximate mid-sagittal image was obtained by manually drawing the slice plane through mid-line structures at the level of the interventricular septum. Third, the sagittal plane was moved laterally until the falx cerebri and uninterrupted central canal (at the level of the midbrain) were present in the same plane. In some cases, the volume was tilted slightly around the AP axis until both structures were present in a single plane. This mid-sagittal image was then extracted and rotated around its center so that the anterior and posterior commissures were horizontal. Fig. 1 shows one sample mid-sagittal image processed in this way.

2.3. Callosal segmentation and matching

We employed a *k*-means clustering algorithm which groups image voxels into k clusters by minimizing the intensity variance within each cluster (Machado and Gee, 1998). Because the performance of this algorithm was highly dependent on the brightness of the input image and number of clusters, we opted to perform cluster segmentation on the same data set using $k = 3$, 4, and 5 and scaled at multiple brightness levels. This process yielded 18 sets of segmentation images (3 segmentation levels $\times$ 6 brightness settings). For each mid-sagittal image, the best segmentation image from the set of 18 was chosen and modified so that the callosa was completely separated from surrounding

structures. The modified image was then used to extract the corpus callosum from the mid-sagittal section. Fig. 1 shows one sample segmentation image.

Once we have generated the set of segmented callosa, our next step was to crop the images and perform registration and deformation to a single template callosum. We want to find a vector field that smoothly maps the image I_1 to image I_2, such that the borders and interiors of the anatomy are well matched. The registration method begins by extracting the boundary of each segmented callosa. A spline is then used to parameterize the boundary points as curves, allowing us to reliably compute various geometric features with which the correspondence or similarity between a curve pair is determined. The registration seeks a smooth reparameterization of the template callosal curve that maximizes its geometric correspondence with the subject curve (Avants and Gee, 2002). This boundary correspondence is then extrapolated to the body of the template and subject callosa through linear interpolation.

2.4. Statistical analysis of the Jacobian

The set of interpolated transformations for all subjects was converted into Jacobian determinant maps, where the Jacobian, J, is defined pointwise as

$$\left|\frac{\partial T_s}{\partial \mathbf{x}}\right|, \tag{1}$$

where $T_s(\mathbf{x})$ is the transformation that takes voxel, $\mathbf{x}$, in the template image to the corresponding voxel in the image of subject s. T_s can be visualized as a vector field of displacements indicating directly the position to which each template voxel is transformed. J then provides a measure of vector "splay" at each voxel and so, describes the size change required in the registration at each point. Values greater than 1 mean regional expansion in the subject in relation to the template while values less than 1 mean just the opposite. Before proceeding, we normalize the Jacobian by dividing each pointwise value by the sum of all Jacobians, L, for each subject:

$$j = \frac{J}{\sum_{i=0}^{L} J_i}. \tag{2}$$

This scaling procedure accounts for global variation in Jacobian values and allows us to analyze relative rather than absolute size differences in the callosum (Pettey and Gee, 2002). This procedure is particularly important in studying gender-based differences; the size of the corpus callosum is known to vary with overall brain size, and males, in general, have larger brain volumes than females. Because the Jacobian field for each subject is derived with respect to the same template, all subject callosa may be compared to each other, voxel for voxel regardless of their shape. This property allows us to calculate pointwise statistics and create statistical parametric maps (SPMs). In order to compare regional shape variations in two populations, we calculate the t score at each pixel, k,

$$t_k^+ = \frac{\bar{j}_k^m - \bar{j}_k^f}{\sigma_k \sqrt{\frac{1}{N_f} + \frac{1}{N_m}}}, \quad t_k^- = \frac{\bar{j}_k^f - \bar{j}_k^m}{\sigma_k \sqrt{\frac{1}{N_f} + \frac{1}{N_m}}}, \tag{3}$$

where,

$$\sigma_k = \sqrt{\frac{(N_m - 1)\sigma_m^2 + (N_f - 1)\sigma_f^2}{N_m + N_f - 2}}. \tag{4}$$

$\bar{j}_k^m$ and $\bar{j}_k^f$ are the mean normalized Jacobians for the male and female groups at the k^{th} pixel, respectively. σ_m and σ_f are the standard deviations of j_k for males and females, respectively. N_m and N_f are the number of subjects in the male group and female group. We calculate the t score in both directions so that we can differentiate areas of contraction and expansion. The t scores, t_k^+ and t_k^-, may now be converted to P values using the Student t cumulative distribution function and then threshold-plotted over a mask of the template callosum. Because we do not correct for the size of clusters, this pointwise P map is referred to as a raw P value map. The P value map may be viewed as a statistical comparison of two sets (male and female) of Jacobians at each voxel. To aid in viewability, the map is divided into two images, one image showing those voxels which are statistically larger in one group, and the other image showing the opposite.

The raw P value map gives us a rough idea where differences in shape exist, but does not give the statistical significance of clusters.

In order to calculate the P value for each cluster, we used techniques for identifying brain activation in functional MRI and PET scans. To identify statistically significant clusters, we applied an iterative algorithm that repeatedly adjusts the t threshold on the original t field until one of two endpoints is reached: (1) A cluster containing $n_{\max}$ pixels exceeding threshold t is found that is calculated to be statistically significant ($P < 0.05$), or (2) no such clusters are found despite repeated decrements of t. The P value we calculate for a cluster is the probability that such a cluster of t values exceeding a certain threshold could occur through chance. The formulae used to calculate cluster P values may be found in Friston et al. (1994) and Worsley et al. (1996).

To compare age-related changes between male and females, we calculated the pointwise Pearson correlation, r_k, between j_k and age,

$$r_k = \frac{SP}{\sqrt{SS_a SS_{jk}}}, \tag{5}$$

where

$$SP = \sum_{i=0}^{N} a(i) j(i)_k - \frac{\sum_{i=0}^{N} a(i) \sum_{i=0}^{N} j(i)_k}{N}, \tag{6}$$

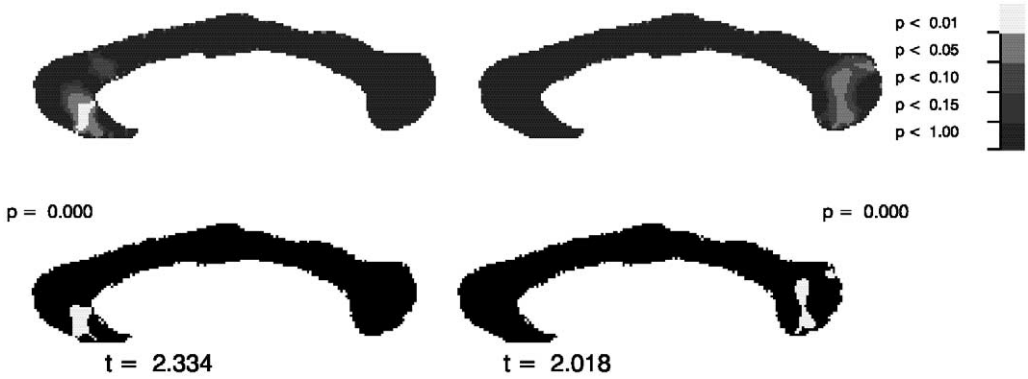

Fig. 2. Size comparison of male and female callosa. Top row displays raw pointwise *P* values and bottom row displays corrected clusters with *P* values. Left side shows areas of larger male size and right shows areas of larger female size.

$$SS_a = \sum_{i=0}^{N} a(i)^2 - \frac{(\sum_{i=0}^{N} a(i))^2}{N}, \quad (7)$$

and

$$SS_{j_k} = \sum_{i=0}^{N} j(i)_k^2 - \frac{(\sum_{i=0}^{N} j(i)_k)^2}{N}. \quad (8)$$

N is the number of subjects in the population, $j(i)_k$ is the normalized Jacobian at the k^{th} voxel in the i^{th} subject. $a(i)$ is the age, in years, of subject i. Positive values for r_k reflect a positive relationship between age and j_k and hence, regional age-related expansion, while negative r_k signifies regional degeneration with age. Pearson fields were generated on the entire population, male and female subgroups, and age-stratified subgroups, as well.

3. Results

Our query of the Schizophrenia Center database yielded a total of 189 cranial MRI's, 94 male and 95 female. The

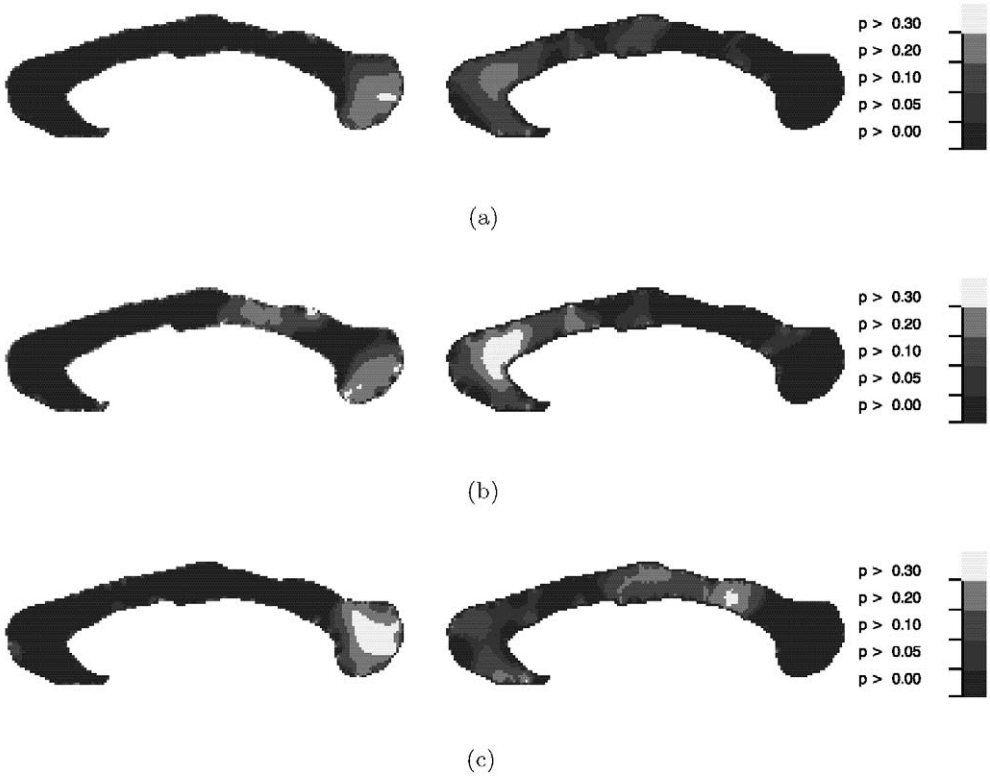

Fig. 3. Pearson plots correlating age with pointwise j_k (normalized). Plot (a) shows analysis for entire population, plot (b) is male only, and (c) is female only. Positive age-related correlation (expansion with age) is shown on the left and negative correlation is displayed on the right.

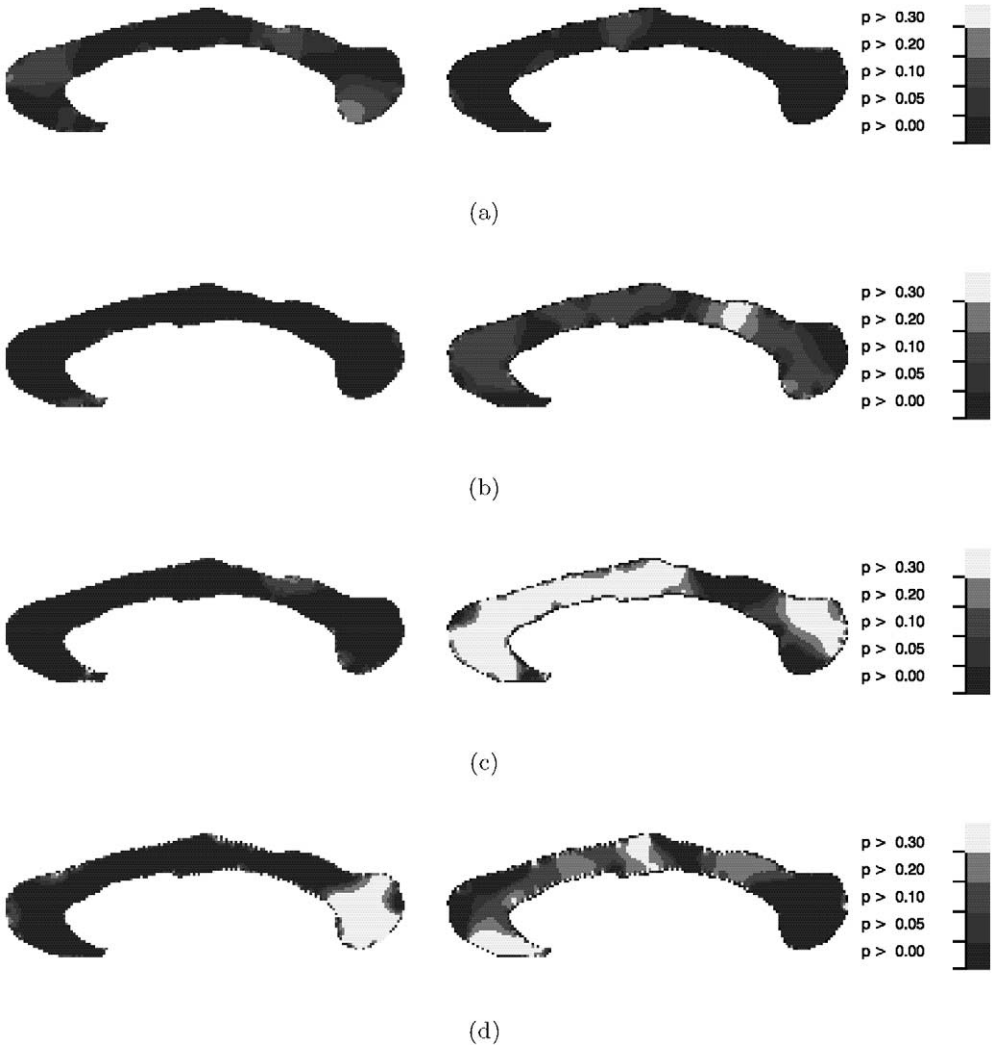

Fig. 4. Pearson plots correlating age with pointwise J_k (nonnormalized) in age-stratified groups. Plots (a) and (b) shows age correlation in male and female subjects 18 to 30 years, respectively. Plots (c) and (d) show age correlation in male and female subjects above 31 years of age, respectively. Positive age-related correlation is shown on the left and negative correlation is displayed on the right.

average age among the male and female subgroups was 29.3 $\pm$ 10 years (range 18 to 84) and 26.8 $\pm$ 9.3 years (range 18 to 74), respectively. Fig. 2 shows the results of the pointwise comparison of mean adjusted Jacobians using raw P values as well as cluster analysis. There is a statistically significant area of expansion in the splenium in females with respect to males ($P < 0.001$) and in the genu of males with respect to females ($P < 0.001$).

Fig. 3 demonstrates the effect of age on pointwise Jacobian values. The aggregate analysis of both genders shows a tendency for splenial expansion and genu contraction with age. Gender stratification revealed that females undergo more age-related splenial expansion than males, while males demonstrate more genu contraction with age.

Figs. 4 and 5 show age-correlation analysis in groups stratified by age using nonnormalized and normalized Jacobians, respectively. Fig. 4 shows that the callosa undergoes very little change in the first three decades of life, male or female. In older subjects, however, there is a substantial region of contraction in the anterior callosa in male subjects, and to a lesser degree in women. Moreover, the splenium of the female callosa expands with age whereas it contracts in males. The normalized plots of Fig. 5 are similar to those of Fig. 4. The anterior callosal contraction, however, is not as impressive.

Changing the template resulted in a slight variation in the exact appearance and location of the aforementioned clusters. Nevertheless, the overall findings of larger female splenium, larger male genu, and reported age-related changes were fairly consistent regardless of template selection.

4. Discussion

Our results with template deformation morphometry demonstrate sexual dimorphism in the splenium of the cor-

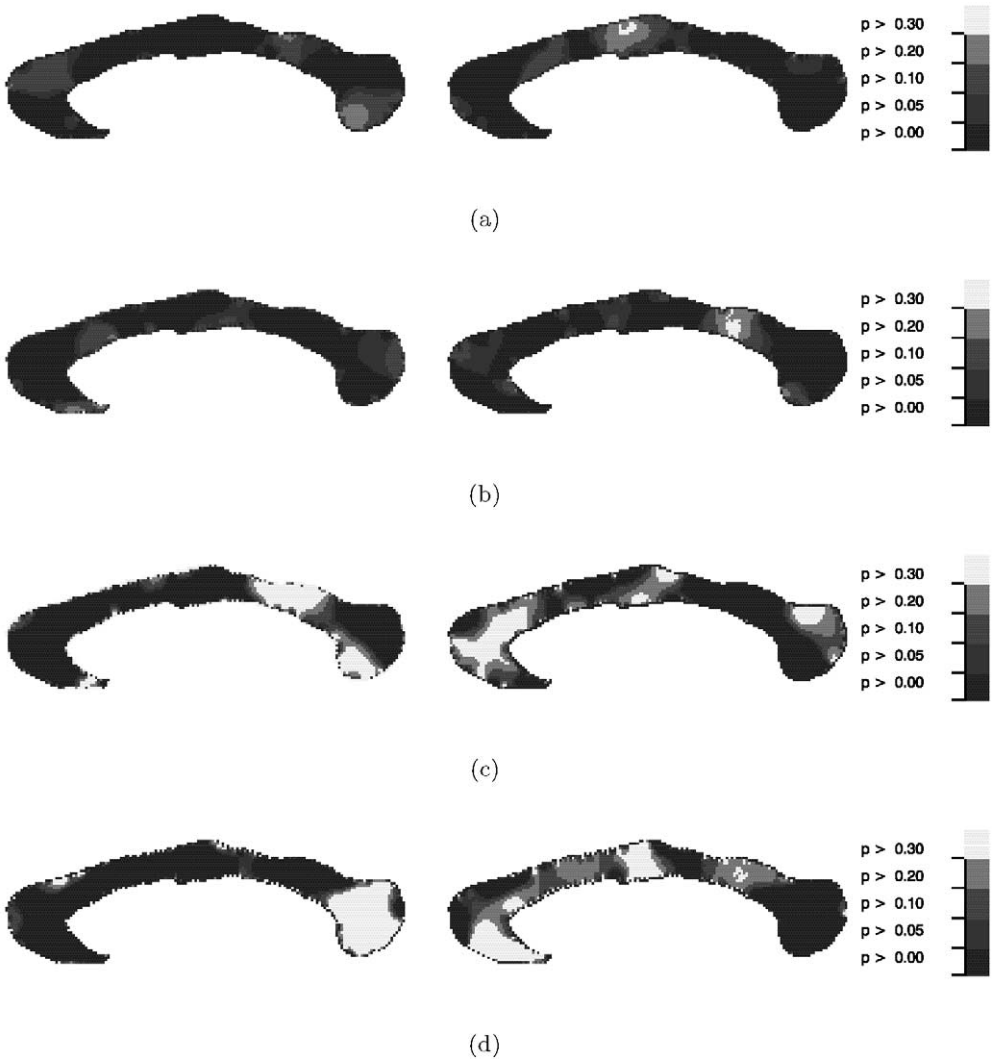

Fig. 5. Pearson plots correlating age with pointwise j_k (normalized) in age stratified groups. Plots (a) and (b) shows age correlation in male and female subjects 18 to 30 years, respectively. Plots (c) and (d) show age correlation in male and female subjects above 31 years of age, respectively. Positive age-related correlation is shown on the left and negative correlation is displayed on the right.

pus callosum. This result is consistent with earlier reports using planimetric methods (Shaywitz et al., 1995). We also found relatively larger genu of the callosum in men, suggesting more bihemispheric communication of the motor tasks likely to be mediated through this region of the callosum. In addition, our results suggest that the female splenium expands with age to a greater degree than the male splenium, while the male genu contracts more than that of the female. Finally, age stratification shows that the majority of neuro-developmental changes in the adult callosa occur after the third decade of life. The major strength of TDM over area-based methods lies in its depiction of voxelwise size differences; we are able to graphically portray regional size differences with a level of detail not possible with other methods. The validity of our results is directly related to the accuracy of our registration method, and so we have made every effort to ensure that our registration compares favorably with human-identified correlations (unpublished data).

Our methods possess some weaknesses. TDM shows shape differences between images and not size differences. The normalization procedure we employ on our Jacobians eliminates global size variation and thus we are limited to examining local shape. This property makes comparison with more traditional cross-sectional area measurements difficult. Because of the uncertainty of normalization which is inherent in absolute size comparisons (Bermudez and Zatorre, 2001), the consideration of shape via TDM may provide a more reliable and meaningful way to analyze structural differences. A second weakness lies in the variation of the results depending on the template used. This, however, is reflected mostly in the variation of the relative statistical significance of a cluster rather than its absolute position in the callosum. Third, the calculation of a point-

wise Pearson correlation assumes a linear relationship between age and Jacobian. This relationship, in actuality, may be much more complicated.

In a similar study using template deformation morphometry, Davatzikos and Resnick (1998) also demonstrated that the splenium was larger in females than males. Their study included an age correlation analysis which showed a tendency toward overall contraction in the callosa in both males and females using nonnormalized Jacobians. This result differs from ours, which shows that the absolute size of the female splenium expands beyond the third decade. This discrepency may be explained by the significantly older age of Davatzikos's subjects. Most of their subjects were older than 70 years, while our sample includes very few participants older than 60.

The findings of the larger female splenium is consistent with the homotopic arrangement of the corpus callosum. The neuropsychological literature indicates enhanced bihemispheric representation of verbal tasks in females (Shaywitz et al., 1995; Gur et al., 2000), and the splenium would be involved in interhemispheric transfer of language processing. The finding of the larger male genu may relate to enhanced motor coordination in men, a finding also supported by the literature (Maccoby, 1966; Joseph and Willingham, 2000, Saykin et al., 1995). The relatively enhanced age-related expansion of the splenium in women (see Fig. 3) suggests that bigger size is due to more protracted development. The present method cannot differentiate between increasing fiber diameter and fiber number as the mechanism of this age-related expansion, but it would be reasonable to posit hormonal differences as the underlying cause. The sensitivity of white matter to metabolic challenge is well known (Yamauchi et al., 2000; Meguro et al., 2000). Thus, we hypothesize that estrogen exerts a positive effect on the callosum or testosterone exerts a negative effect. Still, it is unclear whether enlarged callosal size is causative in the fundamental differences underlying lateralization in males and females. It is possible that preexisting bihemispheric representation of cognitive tasks in women gives rise to a more bulbous splenium or that greater availability of myelinated fibers in the splenium facilitates bihemispheric language representation. Longitudinal studies (Giedd et al., 1999) and studies of young infants (Matsuzawa et al., 2001) may help elucidate the causal direction.

Obtaining a consensus on the subject of sexual dimorphism in the corpus callosum has proven to be elusive using traditional dimensional measures. We offer our results as further proof that sexual dimorphism in the callosum does exist, and these differences may in part be due to a greater age-related expansion of callosal white matter in women.

Acknowledgments

This work was supported in part by the USPHS under Grants NS-33662, LM-03504, MH-62100, AG-15116, AG-17586, and DA-14418.

References

Allen, L., Richey, M., Chai, Y., R., R. G., 1991. Sex differences in the corpus callosum of the living human being. J. Neurosci. 11, 933–942.

Avants, B., Gee, J., 2002. Soft parametric curve matching in scale-space, in: Proc., SPIE Medical Imaging 2002: Image Processing, Bellingham, WA, Vol. 4684, pp. 1139–1151.

Bermudez, P., Zatorre, R.J., 2001. Sexual dimorphism in the corpus callosum: methodological considerations in MRI morphometry. NeuroImage 13, 1121–1130.

Bryden, M.P., 1979. Evidence for sex-related differences in the cerebral organization, in: Wittig, M., Petersen, A.C. (Eds.), Sex-Related Differences in Cognitive Functioning, Academic Press, New York, pp. 121–143.

Davatzikos, C., Vaillant, M., Resnick, S.M., Prince, J.L., Letovsky, S., Bryan, R.N., 1996. A computerized approach for morphological analysis of the corpus callosum. J. Comput. Assist. Tomogr. 20, 88–97.

Davatzikos, C., Resnick, S.M., 1998. Sex differences in anatomic measures of interhemispheric connectivity: correlations with cognition in women but not men. Cereb. Cortex 8, 635–640.

De Lacoste-Utamsing, C.D., Holloway, R., Woodward, D., 1986. Sex differences in the fetal human corpus callosum. Hum. Neurobiol. 5, 93–96.

De Lacoste-Utamsing, C.D., Holloway, R.L., 1982. Sexual dimorphism in the human corpus callosum. Science 216, 1431–1432.

Friston, K.J., Worsley, K.J., Frackowiak, R.S.J., Mazziotta, J.C., Evans, A.C., 1994. Assessing the significance of focal activations using their spatial extent. Hum. Brain Mapp. 1, 153–171.

Giedd, J.N., Blumenthal, J., Jeffries, N.O., Castellanos, F.X., Liu, H., Zijdenbos, A., Paus, T., Evans, A.C., Rapoport, J.L., 1999. Brain development during childhood and adolescence: a longitudinal MRI study. Nature Neurosci. 2, 861–863.

Going, J., Dixson, A., 1990. Morphometry of the adult human corpus callosum: lack of sexual dimorphism. J. Anat. 171, 163–167.

Gur, R., Alsop, D., Glahn, D., Petty, R., Swanson, C.L., Turetsky, J.A.M.B.I., Detre, J.A., Gee, J., Gur, R., 2000. An fMRI study of sex differences in regional activation to a verbal and a spatial task. Brain Lang. 74, 157–170.

Gur, R., Maany, V., Mozley, D., Swanson, C., Bilker, W., Gur, R., 1998. Subcortical MRI volumes in neuroleptic-naive and treated patients with Schizophrenia. Am. J. Psychiatry 155, 1711–1717.

Gur, R., Turetsky, B.I., Bilker, W.B., Gur, R., 1999a. Reduced gray matter volume in Schizophrenia. Arch. of Gen. Psychiatry 56, 905–911.

Gur, R., Turetsky, B.I., Matsui, M., Yan, M., Bilker, W., Hughett, P., Gur, R., 1999b. Sex differences in brain gray and white matter in healthy young adults. J. Neurosci. 19, 4065–4072.

Harshman, R.A., Remington, R., 1976. Sex, language and the brain: a review of the literature on adult sex differences in lateralization. UCLA Working Papers Phonet. 31, 86–103.

Joseph, J.E., Willingham, D.B., 2000. Effect of sex and joystick experience on pursuit tracking in adults. J. Motor Behav. 32, 45–56.

Kimura, D., Harshman, R.A., 1984. Sex differences in brain organization for verbal and non-verbal functions, in: DeVries, G.J., DeBruin, J.P.C., Uylings, H.B.M., Corner, M.A. (Eds.), Sex Differences in Primates, Chap. 61, Elsevier, New York, pp. 423–441.

Maccoby, E., 1966. Development of Sex Differences. Stanford University Press, Stanford.

Machado, A.M.C., Gee, J.C., 1998. Atlas warping for brain mophometry, in: Hanson, K. (Ed.), Proc. SPIE Medical Imaging 1998, volume 3338, Imaging Processing, Bellingham, WA, pages 642–651.

Machado, A.M.C., Gee, J.C., Campos, M.F.M. 2000. A factor analytic approach to strucural characterization, in: Mathetmatical Methods in

Biomedical Image Analysis, pages 219–226, Los Alamitos, CA. IEEE Computer Society.

Matsuzawa, J., Matsui, M., Konishi, T., Noguchi, N., Gur, R., Bilker, W., Miyawaki, T., 2001. Age-related volumetric changes of brain gray and white matter in healthy infants and children. Cereb. Cortex 11, 335–342.

McGlone, J., 1980. Sex differences in human brain asymmetry: a critical survey. Behav. Brain Sci. 3, 215–263.

Meguro, K., Courtheoux, J.M.C.P., Theron, J., Viader, F., Yamadori, A., 2000. Atrophy of the corpus callosum correlates with white matter lesions in patients with cerebral ischaemia. Neuroradiology 42, 413–419.

Pettey, D.J., Gee, J.C., 2002. Sexual dimorphism in the corpus callosum: a characterization of local size variations and a classification driven approach to morphometry. NeuroImage 17, 1504–1511.

Saykin, A., Gur, R., Gur, R., Shtasel, D., Flannery, K., Mozley, L., Malamut, B., Watson, B., Mozley, P.D., 1995. Effects of age, education, gender and ethnicity. Appl. Neuropsychol. 2, 79–88.

Shaywitz, B., Shaywitz, S., Pugh, K., Constable, R., Skudlarski, P., Fulbright, R., Bronen, R., Fletcher, J., Shankweiler, D., Katz, L., 1995. Sex differences in the functional organization of the brain for language. Nature 373, 607–609.

Shtasel, D.L., Gur, R., Mozley, P.D., Richards, J., Taleff, M.M., Heimberg, C., Gallacher, F., Gur, R., 1991. Volunteers for biomedical research: recruitment and screening of normal controls. Arch. Gen. Psychiatry 48, 1022–1025.

Weis, S., Weber, G., Wenger, E., Kimbacher, M., 1989. The controversy about a sexual dimorphism of the human corpus callosum. Intern. J. Neurosci. 47, 169–173.

Witelson, S., 1985. The brain connection: the corpus callosum is larger in left-handers. Science 229, 665–668.

Worsley, K.J., Marrett, S., Neelin, P., Vandal, A.C., Friston, K.J., Evans, A.C., 1996. A unified statistical approach for determining significant signals in images of cerebral activation. Hum. Brain Mapp. 4, 58–73.

Yamauchi, H., Fukuyama, H., Nagahama, Y., Oyanagi, C., Okazawa, H., Ueno, M., Shio, J.K.H., 2000. Long-term changes of hemodynamics and metabolism after carotid artery occlusion. Neurology 54, 2095–2102.

Yoshi, I., Barker, W., Apicella, A., Chang, J., Sheldon, J., Duara, R., 1986. Measurements of the corpus callosum on magnetic resonance scans: effects of age, sex, handedness and disease. Neurology 36 (Suppl.), 133.